NASA DEVELOP National Program
Virginia – Langley

Spring 2024

Cape Hatteras Ecological Conservation

Delineating Shoreline and Mapping Change Along the Cape Hatteras National Seashore for Coastline Management and Transportation Corridor Adaptation Strategies

DEVELOP Technical Report

March 29th, 2024

Ella Haugen (Project Lead)
Alyson Bergamini
Julian Alcantara

Advisors:
Dr. Kenton Ross, NASA Langley Research Center (Science Advisor)
Dr. Xia Cai, NASA Langley Research Center (Science Advisor)

Lead:
Olivia Landry (Virginia – Langley)

1. Abstract

The National Park Service at Cape Hatteras National Seashore works to protect North Carolina's Outer Banks where frequent storms bring heavy winds and flooding, leading to overwash events on the main highway, North Carolina Highway 12. Shorelines are susceptible to erosion directly affecting transportation and housing infrastructures. Storm events can disrupt transportation on NC-12 and ferry service from Ocracoke Island to Hatteras Island, leaving inhabitants stranded on Ocracoke Island for indefinite amounts of time. The National Park Service's current decision-making practices involve mitigating infrastructure damage by enlisting the help of North Carolina's Department of Transportation and finding ways to relocate this infrastructure, as well as dredging and sediment placement that support beach nourishment efforts. Our NASA DEVELOP team partnered with the National Park Service to explore the use of electro-optical data to delineate shoreline and map coastline change from 2014 to 2024. We used Earth observations collected by Landsat 8 Operational Land Imager, Landsat 9 Operational Land Imager-2, and Sentinel-2 MultiSpectral instrument to support decision-making related to prioritizing strategic planning for transportation corridor adaptations including potential relocation of infrastructure, and beach nourishment efforts. We derived coastline maps by consolidating single date images from each year to derive seasonal composite images for assessing winter and summer coastline seasonal oscillation patterns. The results highlight shoreline loss over the ~10-year study period, and the difference in shoreline inundation in the winter and summer seasons. These observations create a better understanding of storm damage mitigation efforts and help the National Park Service to plan for infrastructure updates.

Key Terms

remote sensing, Landsat, Sentinel, barrier island, coastal erosion, road damage, Hurricane Dorian

2. Introduction

2.1 Background

Established as the first national seashore in 1937, Cape Hatteras National Seashore (CAHA) is a historical and cultural landmark that comprises about 70 miles of the Outer Banks in North Carolina. CAHA's mission is to maintain the delicate barrier island processes that shape the ever-changing landscape and protect the several unique species of native plants and animals that inhabit the area. Frequent storms and other natural coastal phenomena have continuously altered the seashore since its induction into the National Park Service (NPS). In addition to the various processes that shape the coast, there have been many human interventions to protect the integrity of the barrier islands, such as the creation of artificial dunes, dredging efforts, and more.

CAHA's geographic location on the Atlantic coast makes the locale susceptible to storms and seasonal winds. In their study of historical wave height changes off the coast of the Carolinas, Komar and Allen (2008) analyzed data from three buoys and determined that waves during the hurricane seasons have significantly increased in both height and frequency since the 1970s. The change in wave characteristics caused progressively drastic effects on the shape of CAHA's coast. Waves from hurricanes have driven widespread changes in erosion rates between the northern and southern flanks of CAHA, which has yielded a more asymmetrical shoreline (Moore et al., 2013). Hurricane Dorian, the most recent powerful storm, hit the Atlantic coast in September 2019 as a Category 1 hurricane and caused significant damage to CAHA. Winds reached 98 mph and inundation levels occurred up to 7 ft, making North Carolina Highway 12 (NC-12) inaccessible, and trapping Ocracoke residents on an isolated island (Avila et al., 2020). While certain winds and storm conditions impose heightened threats to the seashore seasonally, the entire barrier islands are still vulnerable to adverse weather effects year-round.

The United States Geological Survey (USGS) used a Coastal Vulnerability Index to assess CAHA's relative vulnerability, and their findings suggested that more than 50% of the Outer Banks' shoreline is either highly or very highly vulnerable, and another 27% of the shoreline is moderately vulnerable (Pendleton et al., 2004). The vulnerability of the Outer Banks' shorelines indicates potential issues with the area's infrastructure

including the main highway, NC-12. Due to the extent of the area's vulnerability, we examined the entirety of CAHA, with focus on four hotspots requested by our NPS partners: Rodanthe, Avon, Buxton, and northern Ocracoke (Figure 1).

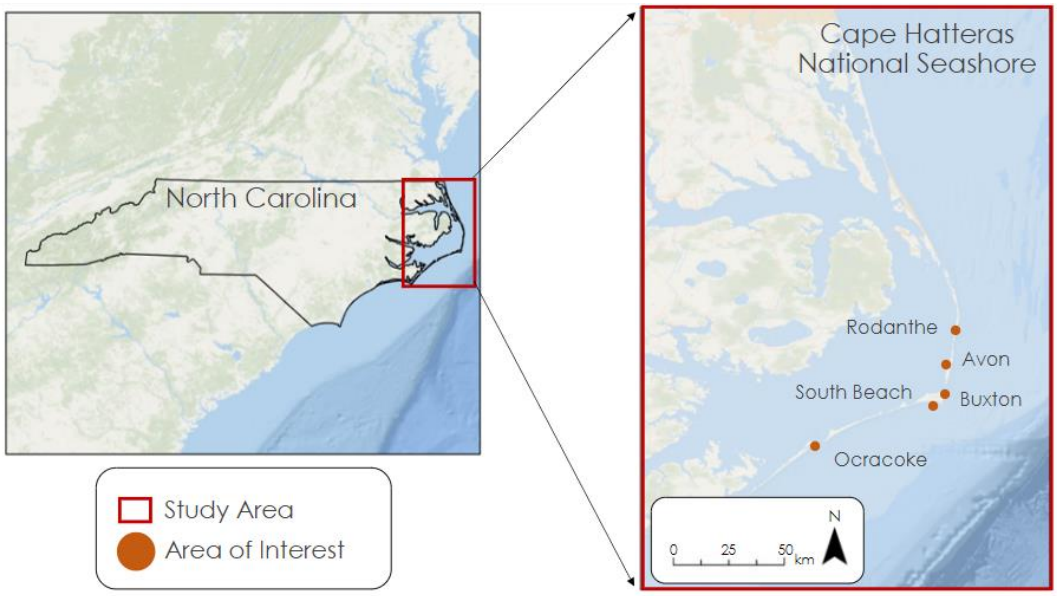

Figure 1. Cape Hatteras National Seashore, shown in relation to the seashore's location in North Carolina and marked with significant locations addressed in this study.

2.2 Project Partners and Objectives

We partnered with the NPS in our effort to monitor shoreline changes at CAHA. The NPS oversees the preservation of the seashore's resources, monitors coastal hazards such as erosion, inundation, and sea level rise, and provides educational information services for visitors. Past research by the NPS focused on coastal resilience, vulnerability, and management using the Digital Shoreline Analysis System, developed by the USGS (Flynn et al., 2021; 2023). The NPS primarily used aerial and field survey data, supplemented by limited use of high-resolution satellite imagery in this research to calculate shoreline change rates. The NPS used these data sources to support transportation infrastructure management recommendations and communication with the Department of Transportation. However, these methods of data collection have limitations. The NPS currently only records data during the spring and autumn, despite the annual sea level extremities occurring during the summer and winter. To create a more complete understanding of seasonal oscillation, the NPS is interested in exploring the feasibility of using NASA electro-optical data.

Widespread availability of freely accessible Earth observations greatly advanced the application of remote sensing techniques in conservation studies. Utilizing multitemporal Landsat satellite data, Mullick et al. (2020) accurately mapped and quantified the change in shoreline for a 240 km stretch of Bangladesh's coast over the span of 40 years. Bernier et al. (2021) also utilized Landsat satellite data to assess the impacts of storms and human alterations on the northern Chandeleur Islands barrier system. To accomplish a similar task for CAHA, the NPS can benefit from employing Landsat 8 OLI and Landsat 9 OLI-2, and Sentinel-2 MSI. Furthermore, by adjusting visual bands of satellite imagery, several useful indices, such as the Modified Normalized Difference Water Index (MNDWI), could aid in differentiating between water and land (Devkota et al., 2023). These methods of data acquisition and processing could vastly increase the NPS' capacity to analyze Earth observations and make more informed decisions in coastline management.

The objectives of this project included: (1) develop an efficient method for analyzing shoreline changes using NASA's Earth observations, (2) identify the regions and infrastructure vulnerable to coastal erosion, and (3) create risk maps to aid the NPS in shoreline conservation efforts. The project identified critical areas of

concern based on the ~ 10-year study period of 2014 to 2024. This project aimed to support decision-making relating to prioritization of investments in mitigation and strategic planning for transportation corridor adaptations including potential relocation of infrastructure.

3. Methodology

3.1 Data Acquisition

To complete a time series of composite images of each study area and highlight the impacts of Hurricane Dorian, we acquired collections of raster images across four satellites: Landsat 8 OLI, Landsat 9 OLI-2, and Sentinel-2 MSI (Table 1). We primarily compared the use of Landsat 8 OLI and Sentinel-2 MSI, and we validated our findings with Landsat 9 OLI-2. We used Google Earth Engine (GEE) to collect and process imagery from our ~ 10-year study period spanning the individual Cape Hatteras area of interest.

Table 1
Landsat 8 OLI, Landsat 9 OLI-2, and Sentinel-2 MSI information

Platform/Sensor	Processing Level	Parameter	Native Resolution	Dates
Landsat 8 OLI	Collection 2 Tier 2	Surface reflectance	30m	4/1/2014 - 2/1/2024
Landsat 9 OLI-2	Collection 2 Tier 2	Surface reflectance	30m	9/27/2021 - 2/1/2024
Sentinel-2 MSI	Harmonized Level-2A	Surface reflectance	10-60m	4/1/2014 - 2/1/2024

3.2 Data Processing

3.2.1 Cloud Masking

We applied cloud filtering and cloud masking functions to the image collections. This filtering, supplied by GEE, identified and selected images that contained less than a specified percentage of pixels identified as cloud and omitted images that contained more than the specified percentage of cloud pixels. The threshold that filtered images varied by dataset (0-8%). The masking function identified remaining clouds and removed them by making cloudy pixels transparent and excluding them from analysis (Gorelick et al., 2017).

3.2.2 Water Indices

Since this research pertained to shoreline delineation, we converted the raster imagery to a form that allowed for the differentiation of land and water via a remote sensing index (Equation 1 & 2). Therefore, we calculated the Modified Normalized Difference Water Index (MNDWI) to every raster image (Xu, 2006; Devkota et al., 2023; Gao, 1996). We also calculated the Normalized Difference Water Index (NDWI; McFeeters, 1996) to four composite images to help assess our MNDWI data sets (Devkota et al., 2023; Xu, 2006).

$$MNDWI = \frac{GREEN - SWIR}{GREEN + SWIR} \quad (1)$$

$$NDWI = \frac{NIR - GREEN}{NIR + GREEN} \quad (2)$$

Afterward, we applied a threshold to the datasets to create a binary image that stored pixels that were just classified as land and water:

$$\text{“}Water\ Index > 0\text{”} = Water$$
$$\text{“}Water\ Index \leq 0\text{”} = Land$$

3.2.3 Composite Images

We assigned the filtered raster images to collections based on year and season. We averaged all indexed images together within the first year of the study period (April 2014 – April 2015) and the last year of the study period (February 2023 – February 2024) to create composite images that represented the shoreline of CAHA for those respective years. We also averaged all the raster images within each winter and summer of every year of the study period, resulting in 20 seasonal composite images (10 winter and 10 summer images, respectively). We defined winter as November 21 to March 21 and summer as May 21 to September 21. With predominately binary images, intermediate values populated the shoreline representing a change in values between land and water (Figure 2). We exported the imagery from GEE as GeoTIFFs.

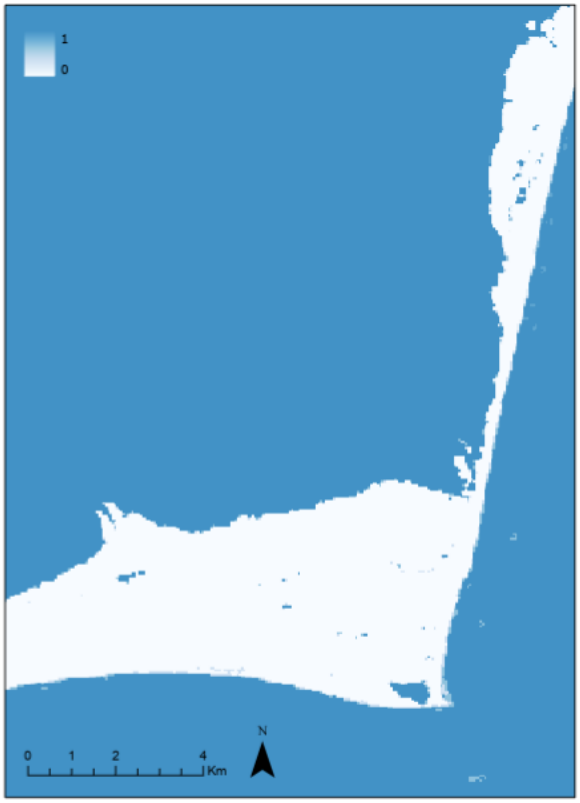

Figure 2. 2023 water/land classification (white (0) = land, blue (1) = water, light blue = coastline/intermediate). Composite image that represents the average shoreline in South Beach and Buxton in 2023.

3.3 Data Analysis

After we completed data processing, we conducted coastal shoreline change analyses. We imported the imagery into ArcGIS Pro and created polygons that encompassed our study areas. The polygons consisted of an "inland" boundary and a buffer that extended seaward 1 km from the inland boundary. We divided each study area polygon into a set of smaller polygons to examine variation within the study area. The smaller polygons were all proportional to each other (within each respective study area). Then, we calculated the sum of the pixels that our classification identified as water within every polygon for every composite image and exported the values to Excel. We converted pixel sum values to area in square meters and used the width of each polygon, which we measured in ArcGIS Pro, to calculate the effective water length of all polygons. The effective water length is a proxy that we created based on the buffer distance into the water. We selected that distance with the purpose of encompassing all shoreline variation. We calculated shoreline change by taking the difference between two effective water length values, which allowed us to quantify the difference between the winter and summer images.

4. Results & Discussion

4.1 Analysis of Results

4.1.1 Rodanthe

The northernmost study area, Rodanthe, is a residential area in which shoreline migration adaptation strategies are well underway. Highway NC-12 used to run parallel to the Eastern shore throughout Rodanthe. Frequent overwash, resulting in road closures and rapid erosion due to its proximity to the westward migrating shoreline, prompted the construction of the Rodanthe bridge, which began in 2018. The bridge opened to traffic in 2022 (Flatiron, n.d.). The bridge carries NC-12 from Rodanthe to the southern point of Pea Island National Wildlife Refuge by going west into the Pamlico Sound and then parallel to an area of the Hatteras Island that is prone to coastal erosion, washouts, and flooding from storms.

We split the Rodanthe study area into two sections: a north section that consisted of a portion of the Pea Island National Wildlife Refuge just north of the Rodanthe bridge, and a south section that encompassed the bridge and Rodanthe. North of the Rodanthe bridge, effective water length tended to decrease during the ~10-year study period, starting at around 903 m in 2014 and decreasing to an average of 885 m in 2023 (Figure 3). This means during the study period, the area gained 18 m of land on average for the surveyed section. In the south section, effective water length tended to increase during the study period, starting at around 890 m and 909 m for summer and winter respectively and increasing to 911 m and 922 m, respectively in 2014 (Figure 3). This means during the summer months the study area lost about 21 m of land and during the winter months the study area lost about 13 m of land. Each of the north and south sub sections saw some variation, but we did not identify a specific pattern (Appendix A). Bridge construction appeared to be in the right place due to the overall land gain north of the bridge and loss parallel to and south of the bridge. The long-term impacts of the bridge construction on overall shoreline loss in the area is a topic for further study.

In Rodanthe, the shoreline oscillates seasonally. On average during the ~10-year study period, the difference between the shoreline in the winter and summer (which is when land loss and gain, respectively, are most extreme) was 10 m. Seasonal oscillation shoreline varied from 5 m to 18 m but did not tend to increase or decrease consistently throughout the study period (Figure 3). Land always increased between the summer and winter, except in the south in 2022. During 2021 and 2022, the Department of Transportation increased sand relocation mitigation efforts.

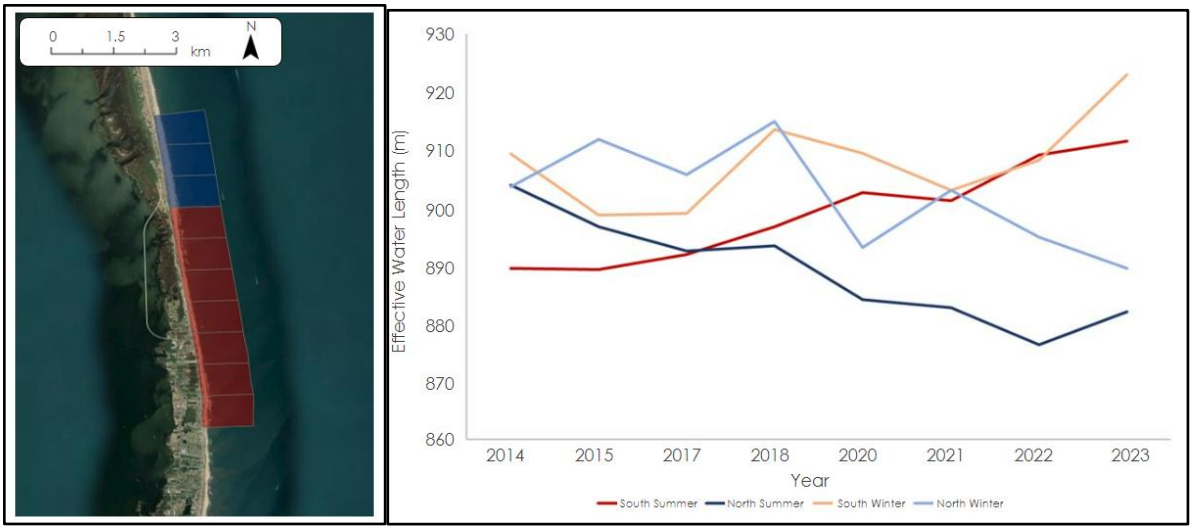

Figure 3. The Rodanthe study area (left). Red polygons represent the south section, which extends from South Rodanthe to the north end of Rodanthe bridge, and blue represents the north section of the study area, which begins where the southern portion ends and extends 2 km north into Pea Island National Wildlife Refuge. Rodanthe's shoreline delineation and seasonal oscillation during the ~10-year study period (right). Orange

and red represent the winter and summer of the south section. Light and dark blue represent winter and summer of the north section.

4.1.2 Avon

The second study area examined for shoreline change, Avon, is a residential area in Cape Hatteras in which shoreline mitigation efforts began and ended in 2022. Avon is situated south of Rodanthe and north of Buxton and Ocracoke, the other study areas. NC-12 runs directly through Avon and is the only route through the area.

We split the Avon study area into two sections based on the average effective water length in each section. The North section encompasses all of Avon north of the fishing pier and as far north as the residential area begins, while the South section includes a small section north of the pier and continues south to the end of the residential area. In the North section of Avon, effective water length tended to decrease during the ~10-year study period, starting at around 854 m in 2014 and decreasing to an average of 833 m in 2023 (Figure 4). This means, during the study period, the area gained about 21 m of land. In the south section, effective water length tended to also decrease during the study period, starting at around 908 m in 2014 and decreasing to 907 m (Figure 4). This means, during the study period, the area appeared to gain about 1 m of land.

Avon's shoreline change remained steady, even gaining land, over the ~10-year study period (Figure 4). These findings could suggest that the mitigation efforts in Avon were successful. The mitigation efforts in Avon proved successful according to the data in the graph. The seasonal oscillation of the shoreline in Avon also showed little change between winter and summer. In 2023, for example, the seasonal oscillation of the north and south areas only saw an increase in effective water length, between winter and summer, of less than 7 m (Appendix B). Viewing this data may help encourage similar mitigation efforts in other areas of CAHA which see more drastic shoreline change.

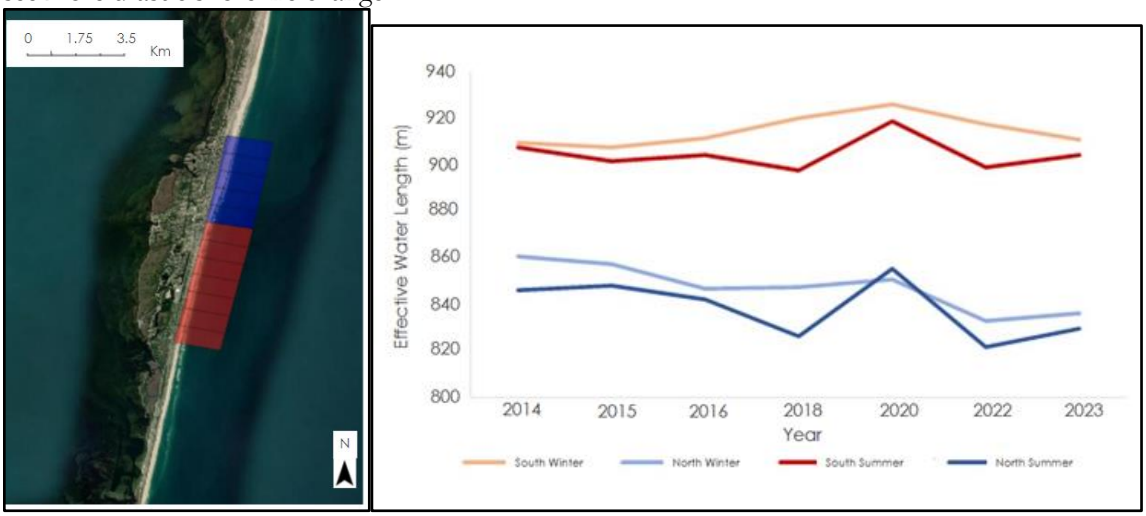

Figure 4. The Avon study area (left). Red polygons represent the south section, which extends from a small section north of the pier and continues south to the end of the residential area, and blue represents the north section of the study area, which begins where the southern portion ends and extends as far north as the residential area begins. Avon's shoreline delineation and seasonal oscillation during the ~10-year study period (right). Orange and red represent the winter and summer of the south section. Light and dark blue represent winter and summer of the north section. Note: 2016's north summer data is only taken from polygons without cloud cover and is therefore missing information from three polygons.

4.1.3 Buxton and South Beach

The third study area examined for shoreline change comprised of Buxton and South Beach, which flank CAHA's point on the east and south, respectively. Buxton is a residential area and the original location of the Cape Hatteras Lighthouse. Due to the threat of shoreline erosion, the lighthouse was moved about 885 m

south in 1999. We evaluated Buxton and South Beach separately due to their differences in geomorphological behavior over the study period, specifically the changing curvature of South Beach's coast and Cape Point's eastward migration.

We divided Buxton into three areas based on shoreline behavior and visualized the changes in effective water length for the northern, middle, and southern portions (Figure 5). The northern and southern portions lost averages of about 5.7 m and 11.5 m of effective water length across their polygons, respectively (Appendix C), meaning both of those areas gained land. Conversely, the middle portion lost land with an increase in effective water length of an average of about 5.6 m.

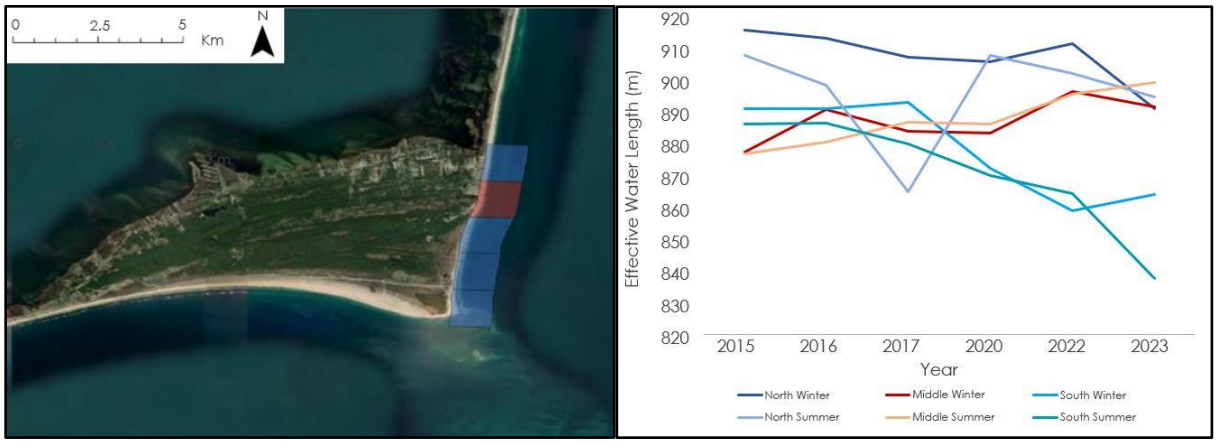

Figure 5. The Buxton study area (left). Buxton's shoreline delineation and seasonal oscillation during the ~10-year study period (right). Blue lines represent the northern and southern portions of the study area that experienced a net gain of shoreline over the study period. The red and orange lines represent the middle section of Buxton that saw a net loss of shoreline.

South Beach exhibited contrasting changes in effective water length across its shoreline. The western portion gained an average of 80.8 m of land across its polygons, while the eastern portion experienced a tremendous loss of about 272.3 m of land as the cape point migrated east (Figure 6). The eastward shift of the point could be attributed to several severe storms that passed over CAHA during the study period. As with the rest of the study areas, South Beach displayed a potential seasonal oscillation as the western portion's effective water length during the winter averaged about 36 m greater than that in the summer, and the eastern portion varied by about 27 m between seasons (Appendix D).

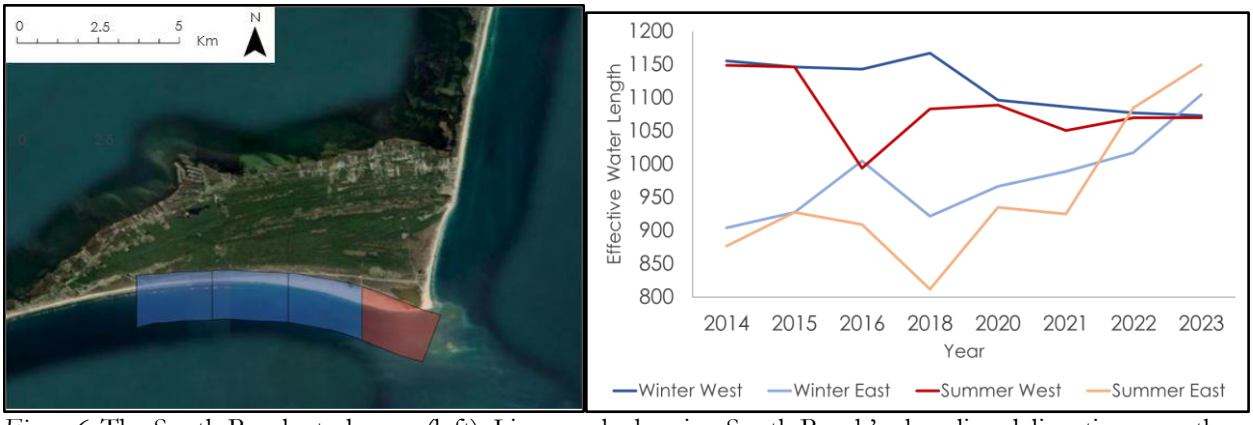

Figure 6. The South Beach study area (left). Line graph showing South Beach's shoreline delineation over the ~10-year study period, as well as displaying the seasonal oscillation between winter and summer each year (right). The blue lines represent the western portion of South Beach that experienced land gain, while the red

and orange lines represent the eastern portion that lost land. The polygons for this location extended 2 km into the ocean to account for the curved beach and ensure all land in the area was covered.

4.1.4 Hurricane Dorian Case Study

Hurricane Dorian devastated CAHA in September 2019. To identify areas most affected by the storm, we distinguished land from water by analyzing NDWI processed images. Areas near Ocracoke and Hatteras Inlets experienced widespread land loss and inundation (Figure 7). Ocracoke Inlet separates Portsmouth Island to the west from Ocracoke Island to the east, and Hatteras Inlet separates Ocracoke Island to the west from Hatteras Island to the east. The only mode of transportation between these islands is by passenger ferry. Due to the frequency and severity of storm conditions in this area, transportation infrastructures are often disrupted, leaving residents stranded on a flooding island. Once the impact areas were established, a similar process was applied to this case study as was to the smaller study areas.

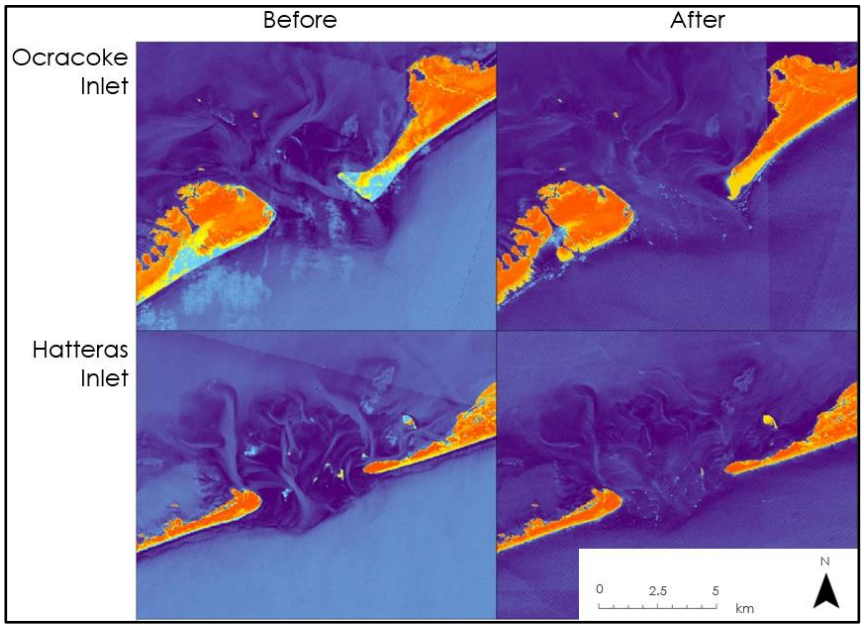

Figure 7. Images of Ocracoke and Hatteras Inlets, before and after Hurricane Dorian, processed through a NDWI to examine changes in shoreline.

Ocracoke Island and the northern end of Portsmouth Island were both divided into four polygons that extended 2 km into the ocean (Figure 8). Ocracoke Island saw an average land loss of about 37 m across the entirety of its Atlantic shore, with the most dramatic change of about 57 m occurring at the southern tip. Portsmouth Island lost an average of about 161 m of land across the polygons, as storm surges connected to the inland marsh areas.

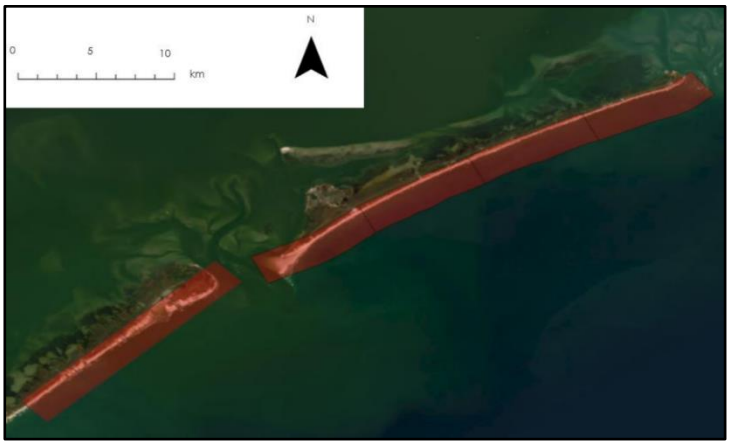

Figure 8. Hurricane Dorian case study area. This map featured the north end of Portsmouth Island and Ocracoke Island, overlaid with red polygons used to analyze shoreline change.

4.1.5 Error Analysis

Throughout this study, we have identified areas in which error could have been introduced into the methodology and resulting end products. First, due to our use of Landsat satellites, it is possible that the moderate spatial resolution of 30 m led us to overlook important features that can only be seen on a finer spatial scale. These features could be seen in ortho-rectified aerial imagery such as NAIP which has a spatial resolution of 0.6 to 1 m. However, NAIP imagery is collected less frequently than Landsat imagery. Additionally, we were unable to include all years within our study period due to image clarity issues. For example, if a composite image for a given season was too cloudy or consisted of too many unclear images, we could not accurately calculate the shoreline for that year. Finally, it should be noted that the method we used to construct polygons within each study area was non-standardized. While polygons within each study area were proportional to one another and had equal width, polygon sizes varied across study areas. Moreover, a buffer was set to 1 km for all study areas, but inland border location was subjective and varied across study areas depending on the impacts that we wanted to highlight.

4.2 Feasibility for Partner Use

The NPS could feasibly replicate our method of shoreline change calculation to observe other study areas throughout CAHA. The most limiting element of the process was filtering out cloudy pictures, which ultimately made the sample size of satellite images much smaller than originally anticipated. Despite this hindrance in data acquisition, processing and analyzing the collected images provided useful insights into the changing profile of the seashore. Since we acquired and processed our data using GEE, all data that was used in this study is publicly available, so our partners could acquire it on their own. While our partners have no previous experience with GEE, they are familiar with ArcGIS Pro and could conceivably implement our methods within ArcGIS Pro to address their shoreline monitoring needs.

4.3 Future Recommendations

Using our methodology, the future incorporation of remotely sensed imagery with higher spatial resolution can provide more accurate classifications of shoreline change. Additionally, Sentinel-1 C-Synthetic Aperture Radar data could be incorporated since our research focused primarily on electro-optical data (e.g., Landsat). The study areas in this project focused primarily on the Atlantic coast of CAHA and on transportation infrastructure (NC-12). Next term, this study could be replicated with additional study areas in CAHA, or it could be applied to the same study areas but with a focus on the sound side of the seashore rather than the Atlantic side. Additionally, other forms of vulnerable infrastructure could be examined, such as residential infrastructure. The application of our methodology using higher resolution commercial satellite data including data available from Maxar WorldView 2 and 3 in new study areas may yield more accurate results that can better inform decision making in the area.

5. Conclusion

In this study, our NASA DEVELOP team partnered with the NPS at CAHA to explore the use of optical data to delineate shorelines and map coastline change over the past ~10 years. We also focused on four specific study areas which included: Rodanthe, Avon, Buxton, and North Ocracoke. Of the study areas, southern Rodanthe showed a land loss of about 17 m, prompting North Carolina's Department of Transportation to build new infrastructure in the form of the Rodanthe bridge to address this issue. Cape Point also saw significant change, accounting for 272 m of land loss highlighted by the migration of the cape. These findings agree with the partners' observations and focus areas for mitigation efforts. The study area of Avon showed the least amount of change, and even saw land gain in both sections, which is probably due to successful mitigation efforts completed in 2022 by CAHA.

The use of Landsat and Sentinel-2 satellite imagery allowed us to download and process relevant data from GEE and analyze that data in ArcGIS Pro. Through raw data and composite images, we analyzed effective water length of the study areas to show shoreline change in terms of land loss or gain. The methodology and tools developed from this project can be easily replicated in the future by our partner for a longer time period and for different study areas on both the Atlantic and Sound sides of North Carolina's barrier islands. They could also allow our partner to view the effects of hurricanes on inlets by visualizing land loss at both sides, as demonstrated the effects of Hurrican Dorian on Hatteras and Ocracoke Inlets. The NPS could use these tools to make effective decisions about shoreline mitigation efforts and infrastructure management decisions, specifically with respect to NC-12.

6. Acknowledgements

The Cape Hatteras Ecological Conservation Team thanks our project partner, the National Park Service at Cape Hatteras National Seashore, especially Michael Flynn for the extensive information and images to help this project find success. In addition, we express gratitude to our science advisors, Dr. Kenton Ross and Dr. Xia Cai, for their support and guidance throughout the project. We also want to thank our node's DEVELOP Leads and Fellows, Olivia Landry, Marisa Smedsrud, and Laramie Plott for keeping us on schedule and supporting us in any way we needed. Finally, we want to thank Mike Ruiz for creating the DEVELOP program and giving us the opportunity to grow our skillsets.

This material contains modified Copernicus Sentinel data (2017-2023) processed by ESA.

Any opinions, findings, and conclusions or recommendations expressed in this material are those of the authors and do not necessarily reflect the views of the National Aeronautics and Space Administration.

This material is based upon work supported by NASA through contract 80LARC23FA024.

7. Glossary

Barrier island – a long, narrow sand island formed by wave and tidal action that is parallel to the mainland and serves to protect the coast from erosion
CAHA – Cape Hatteras National Seashore
Earth observations – Satellites and sensors that collect information about the Earth's physical, chemical, and biological systems over space and time
Effective Water Length – measures the amount of water in meters within a defined area
GEE – Google Earth Engine
MNDWI – Modified Normalized Difference Water Index (derived from the NDWI equation, measures waterbody qualities from satellite data)
MSI – MultiSpectral Instrument
NDWI – Normalized Difference Water Index (highlights waterbody qualities from satellite data)
NPS – National Park Service
OLI – Operational Land Imager, a multispectral sensor aboard the Landsat 8 and 9 satellites

Shoreline change – Difference in effective water length (m)
USGS – United States Geological Survey

8. References

Avila, L.A.; Stewart, S.R.; Berg, R.; Hagen, A.B. National Hurricane Center Tropical Cyclone Report: Hurricane Dorian. Available online: https://www.nhc.noaa.gov/data/tcr/AL052019_Dorian.pdf

Devkota, P., Dhakal, S., Shrestha, S., Shrestha, U.B. (2023). Land use land cover changes in the major cities of Nepal from 1990 to 2020, *Environmental and Sustainability Indicators, 17*(5). http://dx.doi.org/10.1016/j.indic.2023.100227

European Space Agency. (2015). Sentinel 2 Multispectral Imagery (MSI) / Level-2 Surface Reflectance [Dataset]. https://sentinels.copernicus.eu/web/sentinel/user-guides/sentinel-2-msi/processing-levels/level-2

Flatiron Construction Corp. (n.d.). *N.C. 12 Rodanthe Bridge*. Flatiron. https://www.flatironcorp.com/project/n-c-12-rodanthe-bridge/

Flynn, M.J., Allen, T.R., Johnson, M.E., and Hallac, D.E. (2023). Coastal science for resilience and management at the Cape Hatteras National Seashore, NC, USA. *Southeastern Geographer, 63*(1), 54-77. https://doi.org/10.1353/sgo.2023.0005

Flynn, M.J. and Hallac, D.E. (2021). Forecasting oceanfront shoreline position to evaluate physical vulnerability for recreational and infrastructure resilience at Cape Hatteras National Seashore. *Shore & Beach, 89*(2), 97-104. https://doi.org/10.34237/10089211

Gao, B.-C. (1996). NDWI – A Normalized Difference Water Index for Remote Sensing of Vegetation Liquid Water From Space. *Remote Sensing of the Environment, 58*(3), 257-266. https://doi.org/10.1016/S0034-4257(96)00067-3

Gorelick, N., Hancher, M., Dixon, M., Ilyushchenko, S., Thau, D., & Moore, R. (2017). Google Earth Engine: Planetary-scale geospatial analysis for everyone. *Remote Sensing of Environment*, *202*, 18-27. https://doi.org/10.1016/j.rse.2017.06.031

Komar, P. D., & Allan, J. C. (2008). Increasing hurricane-generated wave heights along the US East Coast and their climate controls. *Journal of Coastal Research*, *24*(2), 479-488. https://doi.org/10.2112/07-0894.1

McFeeters, S. K. (1996). The use of the Normalized Difference Water Index (NDWI) in the delineation of open water features. *International Journal of Remote Sensing*, *17*(7), 1425–1432. https://doi.org/10.1080/01431169608948714.

Moore, L. J., McNamara, D. E., Murray, A. B., & Brenner, O. (2013). Observed changes in hurricane-driven waves explain the dynamics of modern cuspate shorelines. *Geophysical Research Letters, 40*(22), 5867-5871. https://doi.org/10.1002/2013GL057311

Mullick, M.R.A., Islam, K.M.A. & Tanim, A.H. (2020) Shoreline change assessment using geospatial tools: A study on the Ganges deltaic coast of Bangladesh. *Earth Science Informatic*s, 13, 299–316. https://doi.org/10.1007/s12145-019-00423-x

Pendleton, E. A., Theiler, E. R., & Williams, S. J. (2005). *Coastal vulnerability assessment of Cape Hatteras National Seashore (CAHA) to sea-level rise* (No. 2004-1064). US Geological Survey. https://pubs.usgs.gov/of/2004/1064/ofr20041064.pdf

U.S. Geological Survey. Landsat 8 Operational Land Imager (OLI) Collection 2, Level 2, Tier 2 Surface Reflectance [Dataset]. Earth Engine Catalog/USGS. Retrieved March 2024, from https://doi.org/10.5066/P9OGBGM6

U.S. Geological Survey. Landsat 9 Operational Land Imager (OLI-2) Collection 2, Level 2, Tier 2 Surface Reflectance [Dataset]. Earth Engine Catalog/USGS. Retrieved March 2024, from https://doi.org/10.5066/P9OGBGM6

Xu, H. (2006). Modification of normalised difference water index (NDWI) to enhance open water features in remotely sensed imagery. *International Journal of Remote Sensing, 27*, 3025-3033. https://doi.org/10.1080/01431160600589179

9. Appendices

Appendix A: Rodanthe

Table A1

Rodanthe average effective water length by section and year and average seasonal shoreline change by year (m)

	South Summer	South Winter	South Shoreline Change	North Summer	North Winter	North Shoreline Change
2014	889.5	909.2	19.7	903.8	903.5	-0.3
2015	889.23	898.7	9.4	896.6	911.7	15.0
2017	891.8	899.0	7.17	892.5	905.6	13.2
2018	896.7	913.4	16.7	893.4	914.8	21.5
2020	902.6	909.4	6.8	884.1	893.0	8.9
2021	901.2	902.9	1.7	882.7	902.9	20.2
2022	909.1	908.1	-0.9	876.3	894.9	18.5
2023	911.4	922.9	11.4	881.9	889.5	7.5

Table A2

Rodanthe average effective water length and average seasonal shoreline change by polygon (m)

	Summer	Winter	Shoreline Change
Poly 1	897.3	907.6	10.4
Poly 2	871.6	878.2	6.7
Poly 3	902.6	909.2	6.6
Poly 4	897.6	905.8	8.2
Poly 5	908.3	912.8	4.5
Poly 6	909.4	917.7	8.3
Poly 7	904.9	918.9	14.0
Poly 8	898.2	913.1	14.9
Poly 9	881.6	899.2	17.6
Poly 10	888.0	899.2	11.3

Appendix B: Avon

Table B1

Avon average effective water length by section and year and average seasonal shoreline change by year (m)

	South Summer	South Winter	South Shoreline Change	North Summer	North Winter	North Shoreline Change
2014	907.9	909.4	1.6	846.4	861.0	14.6
2015	901.6	907.7	6.1	848.2	857.2	9.0
2016	904.3	911.9	7.6	842.0	846.8	4.8
2018	898.1	920.4	22.3	826.6	847.6	21.0
2020	918.7	926.1	7.4	855.8	850.8	-5.0
2022	899.3	917.6	18.3	821.6	832.8	11.2
2023	904.6	910.7	6.1	830.0	836.2	6.2

Appendix C: Buxton

Table C1

South Buxton average effective water length (m)

	South Winer	**South Summer**	**South Shoreline Change**
2015	891.0	885.9	-5.0
2016	891.0	886.4	-4.6
2017	892.9	879.8	-13.2
2020	872.1	869.9	-2.2
2022	858.8	864.3	5.5
2023	864.0	837.4	-26.6

Table C2

Middle Buxton average effective water length (m)

	Middle Winter	**Middle Summer**	**Middle Shoreline Change**
2015	877.1	876.7	-0.5
2016	890.7	880.4	-10.3
2017	883.8	886.6	2.9
2020	883.2	886.0	2.8
2022	896.3	895.3	-0.9
2023	891.6	899.1	7.5

Table C3

North Buxton average effective water length (m)

	North Winter	**North Summer**	**North Shoreline Change**
2015	915.5	907.6	-7.9
2016	913.1	898.2	-14.9
2017	907.2	864.7	-42.5
2020	905.7	907.6	1.9
2022	911.3	902.0	-9.3
2023	890.8	894.5	3.7

Appendix D: South Beach

Table D1

South Beach average effective water length (m)

	West Winter	**West Summer**	**West Shoreline Change**	**East Winter**	**East Summer**	**East Shoreline Change**
2014	1155.6	1149.1	-6.5	904.7	877.3	-27.4
2015	1146.2	1146.2	0.0	928.0	928.0	0.0
2016	1143.4	993.8	-149.6	1005.2	909.4	-95.8
2018	1167.0	1082.8	-84.2	921.4	812.1	-109.3
2020	1096.7	1089.3	-7.4	966.5	934.9	-31.6
2021	1086.1	1050.5	-35.7	989.3	925.0	-64.4
2022	1077.3	1069.8	-7.5	1017.5	1085.0	67.5
2023	1073.4	1069.7	-3.7	1104.8	1149.5	44.7